Available online at www.sciencedirect.com
ScienceDirect
Journal of Nuclear Materials 357 (2006) 156–168
journal of nuclear materials
www.elsevier.com/locate/jnucmat

Mechanical properties of neutron-irradiated nickel-containing martensitic steels: I. Experimental study

R.L. Klueh [a,*], N. Hashimoto [a], M.A. Sokolov [a], K. Shiba [b], S. Jitsukawa [b]

[a] Oak Ridge National Laboratory, P.O. Box 2008, MS 6151, Oak Ridge, Tennessee 37831-6151, USA
[b] Japan Atomic Energy Research Institute, Tokai-mura, Naka-gun, Tokai, Ibaraki 319-1195, Japan

Received 14 November 2005; accepted 17 May 2006

Abstract

Tensile and Charpy specimens of 9Cr–1MoVNb (modified 9Cr–1Mo) and 12Cr–1MoVW (Sandvik HT9) steels and these steels doped with 2% Ni were irradiated at 300 and 400 °C in the High Flux Isotope Reactor (HFIR) up to ≈12 dpa and at 393 °C in the Fast Flux Test Facility (FFTF) to ≈15 dpa. In HFIR, a mixed-spectrum reactor, (n,α) reactions of thermal neutrons with ^{58}Ni produce helium in the steels. Little helium is produced during irradiation in FFTF. After HFIR irradiation, the yield stress of all steels increased, with the largest increases occurring for nickel-doped steels. The ductile–brittle transition temperature (DBTT) increased up to two times and 1.7 times more in steels with 2% Ni than in those without the nickel addition after HFIR irradiation at 300 and 400 °C, respectively. Much smaller differences occurred between these steels after irradiation in FFTF. The DBTT increases for steels with 2% Ni after HFIR irradiation were 2–4 times greater than after FFTF irradiation. Results indicated there was hardening due to helium in addition to hardening by displacement damage and irradiation-induced precipitation.

1. Introduction

Irradiation of a ferritic/martensitic steel first wall of a tokamak fusion reactor by 14 MeV neutrons from the deuterium/tritium fusion reaction will cause displacement damage and production of large amounts of transmutation helium (≈10 appm He/dpa) in the steel. Because no fusion reactor or intense 14-MeV neutron source exists, fusion neutron irradiation effects cannot be studied directly at appropriate damage levels. Fission reactors with neutron energies greater than ≈0.1 MeV can be used to study displacement damage. However, helium formed in a fusion reactor first wall is produced by high-energy neutrons ($\gtrsim$ 5 MeV), and in the absence of an intense 14 MeV neutron source, special techniques are required to simulate the simultaneous production of helium and displacement damage.

Simultaneous displacement damage and helium formation can be produced in alloys containing nickel by irradiating in a mixed-spectrum fission reactor, where displacement damage is produced by fast neutrons in the spectrum, and helium forms by a two-step reaction of ^{58}Ni with thermal

* Corresponding author. Tel.: +1 865 574 5111; fax: +1 865 241 3650.
E-mail address: kluehrl@ornl.gov (R.L. Klueh).

0022-3115/$ - see front matter © 2006 Elsevier B.V. All rights reserved.
doi:10.1016/j.jnucmat.2006.05.048

neutrons in the spectrum. Natural nickel contains 68% ^{58}Ni. For steel with ≈2% Ni, irradiation to ≳10 dpa in the mixed-spectrum High Flux Isotope Reactor (HFIR) at the Oak Ridge National Laboratory (ORNL) produces a similar helium to displacement damage ratio (≈10 appm/dpa) as attained in the undoped steel in a tokamak first wall. Below ≈10 dpa, the ratio is somewhat lower.

Previous papers reported on the tensile [1–3] and Charpy [4–7] behavior of commercial 9Cr–1MoVNb (modified 9Cr–1Mo) and 12Cr–1MoVW (Sandvik HT9)[1] steels and these steels with 1% and 2% Ni after irradiation in HFIR, where larger amounts of helium form, and in the Experimental Breeder Reactor (EBR-II) and Fast Flux Test Facility (FFTF), fast reactors where little helium forms. In this paper, results are presented from further studies of these steels irradiated in the FFTF and HFIR.

2. Experimental procedure

Electroslag remelted heats of 9Cr–1MoVNb (≈0.1% Ni) and 12Cr–1MoVW (≈0.5% Ni) steels were prepared by Combustion Engineering Inc., Chattanooga, Tennessee. Similar compositions with 2% Ni, designated 9Cr–1MoVNb–2Ni and 12Cr–1MoVW–2Ni, were also produced. Chemical compositions are given in Table 1.

Sheet tensile specimens 25.4-mm long with a reduced gage section 7.62-mm long by 1.52-mm wide by 0.76-mm thick were machined from 0.76-mm sheet. Miniature (1/3-size) Charpy specimens 3.3 mm × 3.3 mm × 25.4 mm with 0.51-mm-deep notch and 0.05–0.08-mm root radius were machined from 16-mm thick plates.

Steels were irradiated in the normalized-and-tempered condition: austenitization was 0.5 h at 1050 °C followed by a rapid cool in flowing helium gas; tempering was 5 h at 700 °C.

Two irradiation capsules containing sixteen 25.4-mm long specimen positions were irradiated in the HFIR peripheral target positions with specimens at nominal temperatures of 300 and 400 °C. At each position, either four 1/3-size Charpy specimens, four SS-3 tensile specimens, or about 100 transmission electron microscopy (TEM) specimens in a 12Cr steel subcapsule were enclosed in 12Cr steel holders that were then encapsulated in aluminum sleeves. To control the temperature by nuclear heating, the gas gap between the outer diameter of the steel specimen holder and the aluminum sleeve was adjusted to compensate for the variation in nuclear heating rate along the length of the capsule. A thermal gradient of <45 °C was calculated to exist from the interior to the exterior of the Charpy specimens.

Each capsule contained three flux monitors to determine fluence as a function of distance from the HFIR midplane. Total maximum fluence at the midplane was 6.9×10^{26} n/m^2, with a thermal fluence of 3.2×10^{26} n/m^2 (<0.5 eV) and a fast fluence of 1.68×10^{26} n/m^2 (>0.1 MeV). Maximum displacement damage at the midplane was ≈12 dpa. Only specimens at the center position along the length of the capsule received the peak fluence. Therefore, displacement damage and the helium concentration of the specimens varied depending on their position in the capsule relative to the reactor midplane.

Two tensile specimens and 4–6 Charpy specimens of each steel were irradiated. Specimens irradiated at 300 °C were at the ends of the capsules and received 9–10 dpa. Displacement damage in specimens irradiated at 400 °C was 11–12 dpa.

Table 1
Composition of the steels (wt%)

Element[a]	9Cr–1MoVNb		12Cr–1MoVW	
	Standard	2% Ni	Standard	2% Ni
C	0.09	0.064	0.21	0.20
Mn	0.36	0.36	0.50	0.49
P	0.008	0.008	0.011	0.011
S	0.004	0.004	0.004	0.004
Si	0.08	0.08	0.18	0.14
Ni	0.11	2.17	0.43	2.27
Cr	8.62	8.57	11.99	ll.71
Mo	0.98	0.98	0.93	1.02
V	0.209	0.222	0.27	0.31
Nb	0.063	0.066	0.018	0.015
Ti	0.002	0.002	0.003	0.003
Co	0.013	0.015	0.017	0.021
Cu	0.03	0.04	0.05	0.05
Al	0.013	0.015	0.030	0.028
W	0.01	0.01	0.54	0.54
As	<0.001	<0.001	<0.001	<0.002
Sn	0.003	0.003	0.003	0.002
N	0.050	0.053	0.020	0.017
O	0.007	0.006	0.005	0.007

[a] <0.001 B, <0.001 Zr, balance Fe.

[1] The commercial steels modified 9Cr–1Mo and Sandvik HT9 will be referred to by the generic designations 9Cr–1MoVNb and 12Cr–1MoVW, respectively.

Charpy and tensile specimens were also irradiated at ≈393 °C in the FFTF in the materials open test assembly (MOTA), where the temperature of the specimens was monitored and maintained at ±5 °C. Tensile specimens were irradiated to 3.59×10^{26} n/m^2 ($E > 0.1$ MeV), ≈15 dpa, and Charpy specimens were irradiated to 2.99×10^{26} n/m^2 ($E > 0.1$ MeV), ≈12.4 dpa.

Tensile tests were conducted at the irradiation temperature (400 °C for FFTF specimens) in vacuum on a 44-kN Instron universal testing machine at a nominal strain rate of $\approx 4 \times 10^{-4}$ s^{-1}. Charpy specimens were tested on a machine modified to test miniature specimens. Absorbed energy vs. temperature values were fit with a hyperbolic tangent function to permit upper-shelf energy (USE) and ductile–brittle transition temperature (DBTT) to be consistently evaluated. The DBTT was determined at energy levels midway between upper- and lower-shelf energies. Details on test procedure for subsize Charpy specimens have been published [8,9].

The TEM specimens were thinned using an automatic Tenupol electropolishing unit located in a shielded glove box. Disks were examined using a JEM-2000FX (LaB_6) transmission electron microscope. Foil thickness was measured using thickness fringes in order to evaluate quantitative defect density values.

3. Results

3.1. Tensile behavior

Before irradiation, there was little difference in the yield stress and ultimate tensile strength of the respective steels with and without the 2% Ni addition (Table 2). Irradiation in HFIR caused an increase in the 0.2% offset yield stress and ultimate tensile strength, with the largest effect at 300 °C. The 9Cr–1MoVNb–2Ni steel hardened more than 9Cr–1MoVNb, and the 12Cr–1MoVW–2Ni hardened more than 12Cr–1MoVW at both 300 and 400 °C, indicating a possible helium (or nickel)

Table 2
Tensile properties[a] of steels unirradiated and irradiated in HFIR[b] and FFTF[c]

Steel	Irradiation T (°C/dpa/He(appm))	Strength[d] (MPa)		Elongation (%)		$\Delta\sigma_y$ (MPa]
		Yield	Ultimate	Uniform	Total	
9Cr–1MoVNb	300	673	734	3.5	12.3	
HFIR	300/7/7	1078	1078	0.3	6.4	405
	400	633	693	2.5	10.6	
HFIR	400/12/12	772	792	1.1	7.2	139
FFTF	393/15/<3	768	795	1.4	5.3	135
9Cr–1MoVNb–2Ni	300	679	768	3.3	11.0	
HFIR	300/8/68	1234	1241	0.5	6.0	555
	400	645	723	2.7	9.3	
HFIR	400/12/129	958	958	0.4	6.3	313
FFTF	393/15/<3	810	840	1.6	5.8	165
12Cr–1MoVW	300	690	804	5.5	11.7	
HFIR	300/6/11	1135	1150	0.8	5.0	445
	400	665	763	3.7	10.1	
HFIR	400/12/31	1025	1048	0.8	2.6	360
FFTF	393/15/<3	920	973	1.8	5.1	255
12Cr–1MoVW–2Ni	300	641	818	4.0	10.7	
HFIR	300/6/48	1165	1206	2.6	2.9	524
	400	649	781	3.6	10.4	
HFIR	400/12/141	1093	1113	1.0	1.9	444
FFTF	393/15/<3	903	965	1.8	5.4	254

[a] Values are the average of two tests.
[b] Specimens were irradiated in HFIR to 9–10 dpa at 300 °C and 11–12 dpa at 400 °C.
[c] Specimens were irradiated in FFTF to ≈15 dpa at 393 °C.
[d] The test temperature was the same as the irradiation temperature for the HFIR-irradiated specimens; it was 400 °C for the FFTF-irradiated specimens.

effect. Irradiation caused a decrease in uniform and total elongations (Table 2).

After irradiation in FFTF, there was little difference in the increase in yield stress ($\Delta\sigma_y$) of the steels with different nickel concentrations (Table 2). The $\Delta\sigma_y$ for 9Cr–1MoVNb without and with nickel were 135 and 165 MPa, respectively, and for 12Cr–1MoVW without and with nickel were 255 and 254 MPa, respectively.

When the steels irradiated in HFIR and FFTF are compared, there is no difference in yield stress [Fig. 1(a)] and ultimate tensile strength [Fig. 1(b)] of 9Cr–1MoVNb steel irradiated in HFIR and FFTF at 400 and 393 °C, respectively, but the rest of the specimens showed more hardening after irradiation in HFIR. For the yield stress, a 15%, 10%, and 17% difference was observed for the 9Cr–1MoVNb–2Ni, 12Cr–1MoVW, and 12Cr–1MoVW–2Ni steels, respectively. Differences in the ultimate tensile strengths were slightly less.

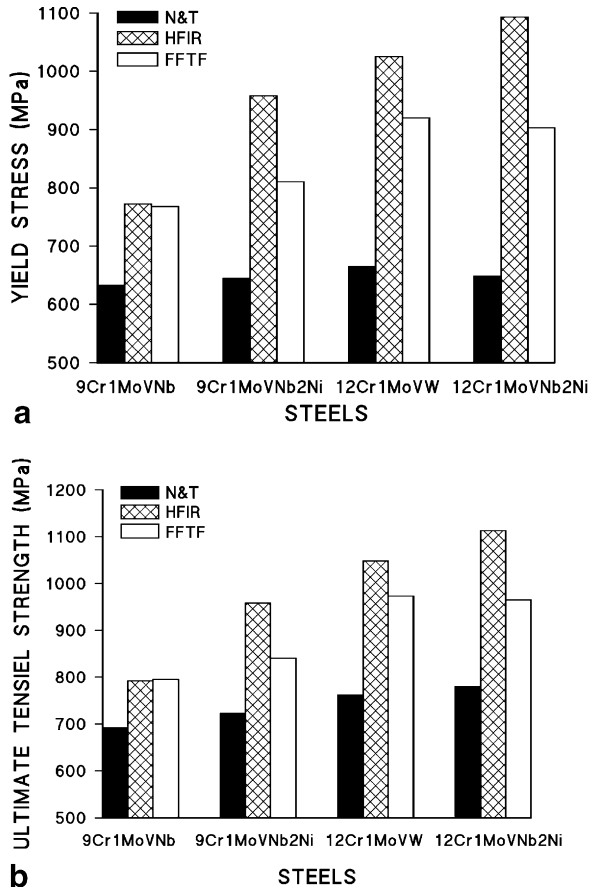

Fig. 1. A comparison of the (a) yield stress and (b) the ultimate tensile strength at 400 °C of steels in the normalized-and-tempered condition and after irradiation in HFIR and FFTF.

3.2. Charpy behavior

Irradiation caused an increase in the DBTT (ΔDBTT) and a reduction in the USE for all specimens irradiated at 300 and 400 °C in HFIR and at 393 °C in FFTF (Table 3). The HFIR results indicated a larger ΔDBTT for steels irradiated at 300 °C than at 400 °C (Fig. 2). Irradiations at 300 °C produced a larger shift in DBTT for the steels with the 2% Ni, with the largest effect occurring for the 9Cr–1MoVNb–2Ni steel, where the shift was over twice that for the steel with no nickel addition. A smaller difference (≈1.4 times) occurred for the 12 Cr steels, where the difference in helium concentration of the two steels was less (Table 1). A similar effect was observed for the steels after irradiation in HFIR at 400 °C, where the ΔDBTT for 9Cr–1MoVNb–2Ni was ≈1.7 times that for 9Cr–1MoVNb and that for 12Cr–1MoVW–2Ni was ≈1.6 times that for 12Cr–1MoVW.

The ΔDBTTs for the 9Cr–1MoVNb steel were similar after irradiation at 400 °C in HFIR and 393 °C in FFTF (Fig. 2). For the 9Cr–1MoVNb–2Ni steel, however, the ΔDBTT after HFIR irradiation at 400 °C was four times greater than after irradiation in FFTF at 393 °C. The ΔDBTTs for the 12Cr–1MoVW and 12Cr–1MoVW–2Ni after irradiation in HFIR at 400 °C were both nearly twice as large as after irradiation in FFTF at 393 °C.

The reduction in USE was generally greater for the steels irradiated in HFIR than FFTF (Fig. 3). The difference in USE between steels irradiated at 300 and 400 °C in HFIR was generally quite small.

3.3. Transmission electron microscopy (TEM) and scanning electron microscopy (SEM)

Specimens of 9Cr–1MoVNb and 9Cr–1MoVNb–2Ni steels irradiated in HFIR at 400 °C were examined by TEM (no TEM was obtained for the 12Cr steels) [10]. Both the 9Cr–1MoVNb and 9Cr–1MoVNb–2Ni steels irradiated in HFIR at 400 °C developed $a_0\langle 1\,0\,0\rangle$ and $(a_0/2)\langle 1\,1\,1\rangle$ dislocation loops with the number density slightly larger and the loops slightly smaller for 9Cr–1MoVNb–2Ni (Fig. 4). Dislocation loop densities and sizes were as follows: $a_0\langle 1\,0\,0\rangle$ were 5×10^{21} m^{-3}, 21 nm and 7×10^{21} m^{-3}, 20 nm for 9Cr–1MoVNb and 9Cr–1MoVNb–2Ni, respectively; $(a_0/2)\langle 1\,1\,1\rangle$ were 4×10^{21} m^{-3}, 25 nm

Table 3
Impact properties of steels unirradiated and irradiated in HFIR[a] and FFTF[b]

Steel, reactor	Irradiation temperature, °C	Transition temperature, °C[c]	ΔDBTT, °C	Upper-shelf energy, J
9Cr–1MoVNb	Unirradiated	−1		10.0
HFIR	300	143	144	4.1
HFIR	400	93	94	5.7
FFTF	393	99	100	6.4
9Cr–1MoVNb–2Ni	Unirradiated	−117		9.0
HFIR	300	181	298	4.0
HFIR	400	47	164	6.3
FFTF	393	−76	41	6.4
12Cr–1MoVW	Unirradiated	−39		7.1
HFIR	300	147	186	3.7
HFIR	400	84	123	3.5
FFTF	393	26	65	4.0
12Cr–1MoVW–2Ni	Unirradiated	−75		6.3
HFIR	300	185	260	3.5
HFIR	400	118	193	3.4
FFTF	393	25	100	4.8

[a] Specimens were irradiated in HFIR to 9–10 dpa at 300 °C and 11–12 dpa at 400 °C.
[b] Specimens were irradiated in FFTF to ≈15 dpa at 393 °C.
[c] Taken at one-half the upper-shelf energy.

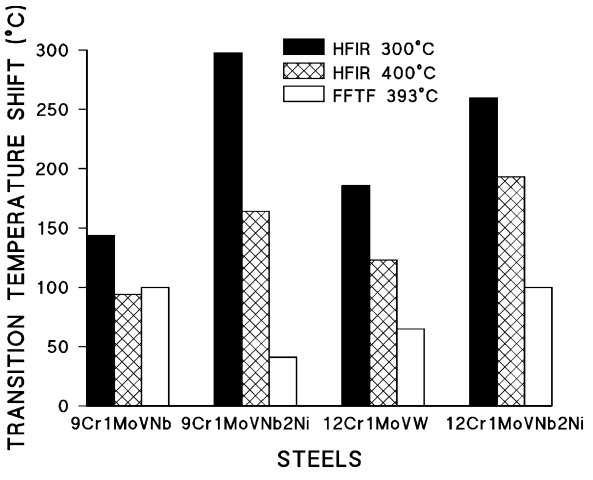

Fig. 2. Shift in ductile–brittle transition temperature of the steels after irradiation in HFIR at 300 and 400 °C and in FFTF at 393 °C.

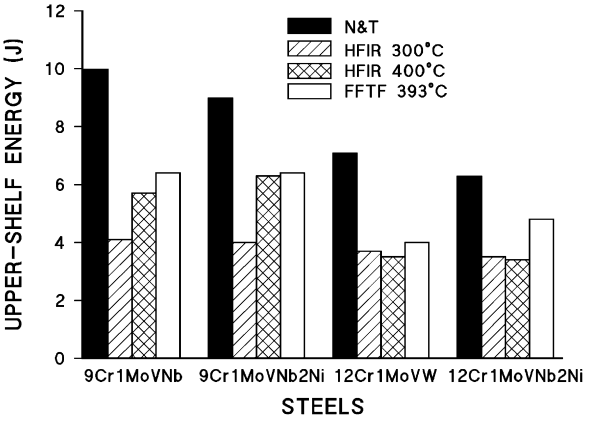

Fig. 3. Upper-shelf energy of the steels in the normalized-and-tempered (unirradiated) condition and after irradiation in HFIR at 300 and 400 °C and in FFTF at 393 °C.

and 6×10^{21} m^{-3}, 24 nm for 9Cr–1MoVNb and 9Cr–1MoVNb–2Ni, respectively.

Cavities also developed, with 9Cr–1MoVNb–2Ni steel having a higher number density (9×10^{21} vs. 3×10^{21} m^{-3}) and smaller average size (5 vs. 9 nm) (Fig. 5). For these low irradiation doses, there was little difference in swelling for the two steels: 9Cr–1MoVNb was estimated at 0.17%, and 9Cr–1MoVNb–2Ni was estimated at 0.15%.

Precipitate microstructures before irradiation consisted primarily of $M_{23}C_6$ on lath and prior-austenite grain boundaries with similar quantities ($<1 \times 10^{20}$ m^{-3}) and average sizes (≈100 nm) in both the 9Cr–1MoVNb and 9Cr–1MoVNb–2Ni steels. There were also a few widely scattered MX particles within the matrix. Irradiation caused little change in the $M_{23}C_6$ structure for either 9Cr steel, and no new precipitates formed in the 9Cr–1MoVNb [Fig. 6(a)]. However, a irradiation-induced precipitate identified as M_2X at a number density of 5×10^{20} m^{-3} and a

mean size of 54 nm was observed in the 9Cr–1MoVNb–2Ni steel [Fig. 6(b)].

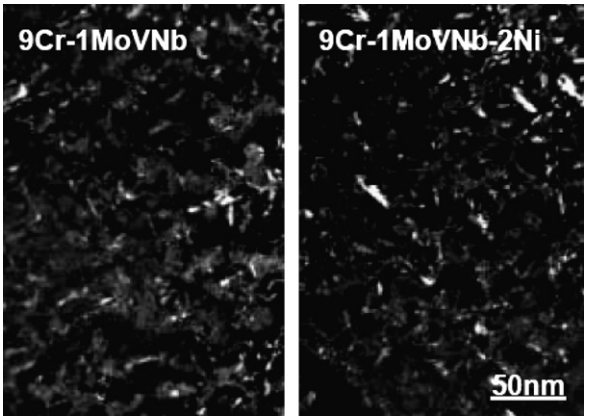

Fig. 4. Dislocation segments and loops in 9Cr–1MoVNb and 9Cr–1MoVNb–2Ni irradiated in HFIR to ≈12 dpa at 400 °C using diffraction conditions: $\mathbf{g} = 110$ ($\mathbf{g}, \mathbf{4g}$).

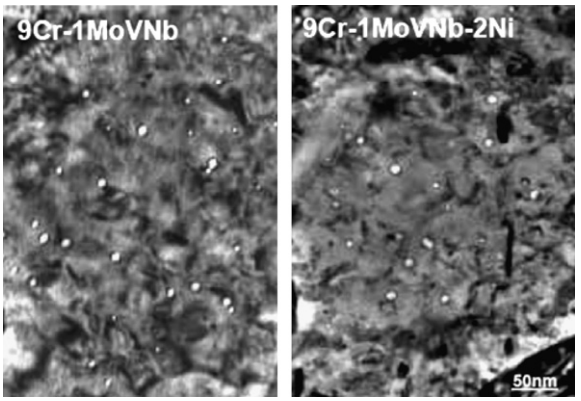

Fig. 5. Cavities in 9Cr–1MoVNb and 9Cr–1MoVNb–2Ni irradiated in HFIR to ≈12 dpa at 400 °C.

Fracture surfaces of Charpy specimens from the lower- and upper-shelf regions of the Charpy curve for each steel were examined by SEM. The fracture surfaces of specimens from lower-shelf regions exhibited typical cleavage fractures, and those from upper-shelf regions exhibited ductile-type shear, which is similar to observations on the surfaces of specimens in the unirradiated condition.

4. Discussion

In previous studies on nickel-doped steels, different tempering treatments were used on the steels with 2% Ni (5 h at 700 °C) and the standard steels (1 h at 760 °C for the 9Cr–1MoVNb and 2.5 h at 780 °C for the 12Cr–1MoVW; these are recommended tempering treatments for commercial 9Cr–1MoVNb and 12Cr–1MoVW steels, respectively) [1–7]. The lower tempering temperature was used for steels with 2% Ni to avoid tempering above A_1, the equilibrium temperature above which ferrite begins to transform to austenite; A_1 is lowered by nickel. An attempt was made to temper to similar room-temperature hardnesses (strengths) using the different tempering conditions. Unfortunately, even though hardnesses were similar for the different tempering conditions, the yield stresses at room temperature and the irradiation temperatures before irradiation turned out to be somewhat different, which complicated the comparison after irradiation [1–7].

For the present experiments, the same tempering treatment was used for all steels (5 h at 700 °C). Although this heat treatment produced similar strengths for all steels at room temperature, 300, and 400 °C, the new tempering conditions changed

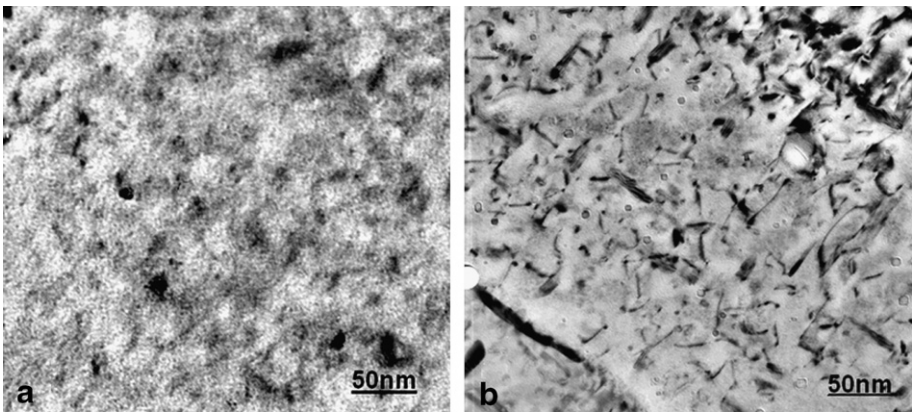

Fig. 6. Precipitates in the matrix of (a) 9Cr–1MoVNb and (b) 9Cr–1MoVNb–2Ni steels irradiated in HFIR to ≈12 dpa at 400 °C.

the DBTTs of the standard steels: the DBTT of the 9Cr–1MoVNb increased from −29 to −1 °C and that for 12Cr–1MoVW decreased from −18 to −39 °C. The steels with 2% Ni had lower DBTTs than the respective steels without the nickel addition. In other words, it was not possible to have both the DBTT and yield stress of the standard steels and the steels with 2% Ni similar prior to irradiation. The lower DBTT for the nickel-containing steels before irradiation (Table 3) reflects the well-known fact that nickel lowers the transition temperature of steels [11].

4.1. Irradiation hardening and embrittlement

When the steels with and without the nickel additions were given the same tempering treatments, they had similar strengths at 300 and 400 °C before irradiation (Table 2). The greater hardening after irradiation in the HFIR at 300 than at 400 °C is expected [1–3]. After irradiation in HFIR, the respective yield stress increases for 9Cr–1MoVNb, 9Cr–1MoVNb–2Ni, 12Cr–1MoVW, and 12Cr–1MoVW–2Ni were respectively 405, 555, 445, and 524 MPa at 300 °C and 139, 313, 360, and 444 MPa at 400 °C. These results indicate a larger increase at both 300 and 400 °C for the steels with 2% Ni than their counterparts without a nickel addition.

After irradiation in FFTF at 393 °C, yield stress increased 135, 165, 255, and 254 MPa for 9Cr–1MoVNb, 9Cr–1MoVNb–2Ni, 12Cr–1MoVW, and 12Cr–1MoVW–2Ni, respectively. With the exception of the 9Cr–1MoVNb, the yield stress increases for the different steels were smaller after FFTF irradiation than after HFIR irradiation (Fig. 1). A similar increase occurred for 9Cr–1MoVNb at 393 °C in FFTF and at 400 °C in HFIR. Since there was only a small difference in displacement damage in the two reactors and hardening saturates with fluence at <10 dpa at ≈400 °C [2,3,12], similar hardening might be expected, as observed for the 9Cr–1MoVNb, because it contains the least nickel and, therefore, the least helium. The 15%, 10%, and 17% higher yield stress in HFIR over that in FFTF for the 9Cr–1MoVNb–2Ni, 12Cr–1MoVW, and 12Cr–1MoVW–2Ni, respectively, are not all that large, especially considering the change in DBTT to be discussed in the next section. However, note that the largest changes are for the steels with 2% nickel and the 12Cr–1MoVW, which contains 0.43% Ni; 9Cr–1MoVNb contains 0.11% Ni (Table 1). This implies that an argument can be made that helium caused much of the difference because, as discussed below, similar precipitate phases are expected during irradiation in the two reactors.

In Fig. 7(a), ΔDBTT is plotted against $\Delta\sigma_y$ for results from irradiation in HFIR at 300 and 400 °C; Fig. 7(b) shows the same data along with data from the FFTF irradiation at 393 °C. The data were fit by linear regression with lines through the origins and had slopes of 0.46 (correlation coefficient $r = 0.94$) and 0.45 ($r = 0.92$), for Fig. 7(a) and (b), respectively. All indications are that the results follow linear relationships, indicating the shift in transition temperature is proportional to hardening.

Fig. 8 shows just the data for the 400 °C irradiations in HFIR and the 393 °C irradiations in FFTF

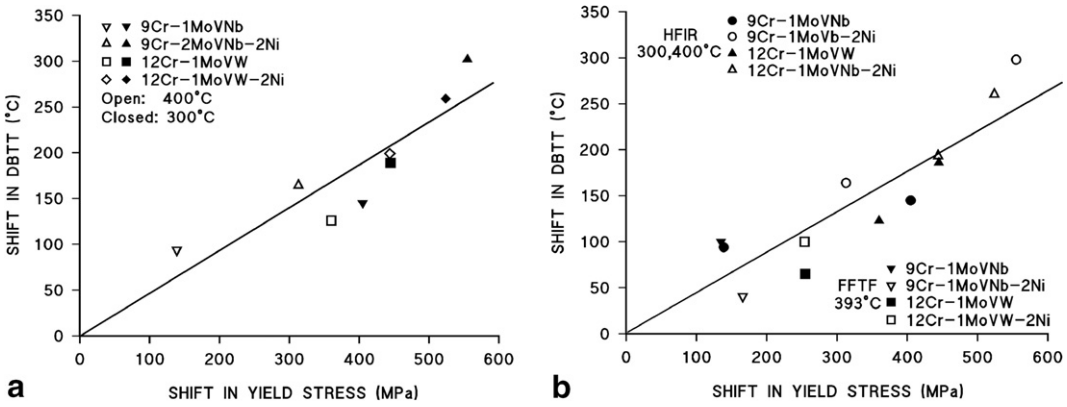

Fig. 7. Shift in ductile–brittle transition temperature plotted against shift in yield stress for 9Cr–1MoVNb, 9Cr–1MoVNb–2Ni, 12Cr–1MoVW, and 12Cr–1MoVW for irradiation in (a) HFIR at 300 and 400 °C and (b) HFIR at 300 and 400 °C and FFTF at 393 °C.

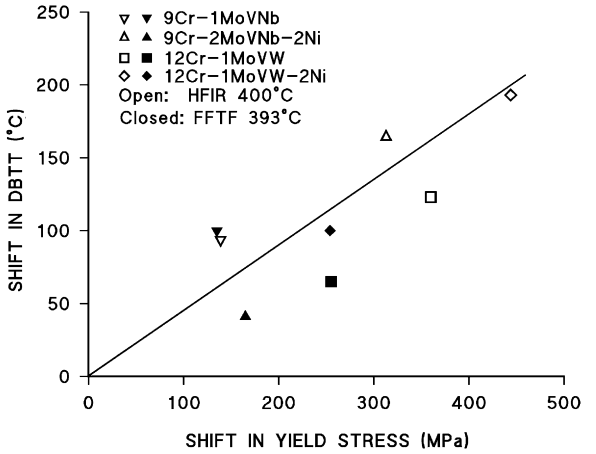

Fig. 8. Shift in ductile–brittle transition temperature plotted against shift in yield stress for 9Cr–1MoVNb, 9Cr–1MoVNb–2Ni, 12Cr–1MoVW, and 12Cr–1MoVW irradiated in HFIR at 400 °C and FFTF at 393 °C.

with a regression line of slope 0.42 ($r = 0.86$). There was both more hardening and a larger shift in transition temperature for the 9Cr–1MoVNb–2Ni, 12Cr–1MoVW, and 12Cr–1MoVW–2Ni steels irradiated in HFIR at 400 °C than in FFTF at 393 °C, even though displacement damage in the two reactors was similar and saturation with fluence would be expected for these doses at these temperatures [2,3,12]. There was no difference for the two reactors for 9Cr–1MoVNb, which contained the least helium after HFIR irradiation.

Although there is no difference between the ΔDBTT for the 9Cr–1MoVNb in FFTF at 393 °C and HFIR at 400 °C in the present irradiations, there are differences for the 9Cr–1MoVNb–2Ni, 12Cr–1MoVW, and 12Cr–1MoVW–2Ni steels (Fig. 8). For the latter three steels, the ΔDBTT values after irradiation in HFIR are 2–4 times greater than in FFTF, which is consistent with a helium effect. This might be expected since the 9Cr–1MoVNb steel contained a calculated value of only about 12 appm He after irradiation in HFIR, compared to ≈31, 129, and 141 for the 12Cr–1MoVW, 9Cr–1MoVNb–2Ni, and 12Cr–1MoVW–2Ni steels, respectively. Thus, a larger effect would be expected for the latter steels if it is a helium effect. Since there was a similar difference in the hardening of the steels depending on the helium concentration, it is concluded that there is a contribution to hardening due to helium that is over and above the hardening due to displacement damage and irradiation-induced precipitation, and that hardening by helium causes a further increase in ΔDBTT after irradiation in HFIR.

After irradiation at 300 °C, where no comparison is possible with irradiation in a fast reactor, the ΔDBTT for the 9Cr–1MoVNb was again the smallest (144 °C), followed by 12Cr–1MoVW (186 °C), 12Cr–1MoVW–2Ni (260 °C), and 9Cr–1MoVNb–2Ni (298 °C). This is also in line with $\Delta\sigma_y$ [Fig. 5] and the amount of helium present in the respective steels (the 9Cr–1MoVNb, 12Cr–1MoVW, 12Cr–1MoVW–2Ni and 9Cr–1MoVNb–2Ni steels contain ≈8, 20, 48 and 47 appm He, respectively).

Tensile and Charpy results from the present HFIR and FFTF irradiations will now be compared to results from previous studies of the same steels irradiated in HFIR and EBR-II (experimental breeder reactor), where it was concluded that helium affected impact properties [2–4,6,7]. One reason for this conclusion is shown in Fig. 9, where ΔDBTT for 9Cr–1MoVNb and 12Cr–1MoVW steels are shown after irradiation in HFIR [6] and EBR-II [12], a fast reactor where little helium forms. After irradiation in EBR-II at 390 °C, the ΔDBTTs after 13 and 26 dpa (<0.1 appm He) were similar, indicating the expected saturation with fluence (ΔDBTT ≈54 °C for the 9Cr–1MoVNb and ≈140 °C for the 12Cr–1MoVW). This saturation did not occur for 9Cr–1MoVNb and 12Cr–1MoVW steels irradiated to ≈40 dpa at 400 °C in HFIR, where ≈30 and 120 appm He formed, and the ΔDBTTs were 207 and 242 °C, respectively. The irradiation-induced

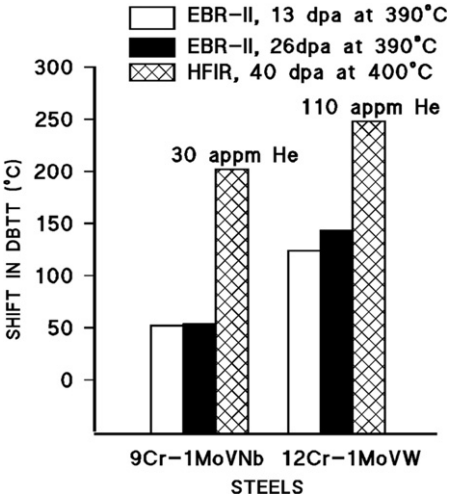

Fig. 9. Shift in ductile–brittle transition temperature for 9Cr–1MoVNb and 12Cr–1MoVW irradiated the HFIR at 400 °C and EBR-II at 390 °C [5].

shift in DBTT after irradiation in EBR-II was attributed to irradiation hardening caused by the dislocation loops from displacement damage and any hardening due to radiation-induced precipitation [6,12]. These processes undoubtedly also occurred during HFIR irradiation, but in this case, there was an additional increment in ΔDBTT that was attributed to helium [6].

Another reason for concluding there was a helium effect was that after the 9Cr–1MoVNb–2Ni and 12Cr–1MoVW–2Ni steels were irradiated in HFIR to ≈40 dpa at 400 °C and ≈400 appm helium, the ΔDBTT values were 348 and 328 °C, respectively [6]. This was over three times the value obtained for 12Cr–1MoVW–2Ni irradiated in FFTF at 390 °C [5], where the ΔDBTT at saturation was 90 °C (9Cr–1MoVNb–2Ni was not irradiated at 390 °C), and it was over 1.5 times that of the steels with no nickel additions (less helium) irradiated in HFIR. Hardening results from the previous irradiations in FFTF agreed with the recent observations on the hardening of the steels irradiated in the fast reactor, that is, steels without nickel showed similar hardening and shifts in DBTT to those with nickel. However, for the HFIR irradiations, there was no additional increment of hardening that could be attributed to helium [3], as was the case in the present experiments.

Specimens were also previously irradiated to ≈27 dpa at 300 °C in HFIR [5]; the helium concentrations were ≈20, 230, 70, and 240 appm for the 9Cr–1MoVNb, 9Cr–1MoVNb–2Ni, 12Cr–1MoVW, and 12Cr–1MoVW–2Ni, respectively. A helium effect was suggested by the larger ΔDBTT for the 9Cr–1MoVNb–2Ni and 12Cr–1MoVW–2Ni steels compared to steels without nickel. Since no fast reactor comparisons are possible for this HFIR-irradiation temperature, these results will not to be discussed further here.

Fig. 10 shows data from Fig. 8 of the present HFIR (HFIR #2) and FFTF experiments at 400 °C to ≈12 dpa and 393 °C to ≈15 dpa, respectively, to which were added data from the previous HFIR (HFIR #1) experiment at 400 °C to ≈40 dpa [2–4,6,7]. The linear-regression line fitting the data from the present HFIR and FFTF irradiations in Fig. 8 is also shown. Although data are limited, the results from the previous experiment deviate significantly from the line obtained for the recent results. For the high-dose data, there is a much larger $\Delta DBTT/\Delta\sigma_y$ compared to the lower-dose data. That is, the previous high-dose data do not appear

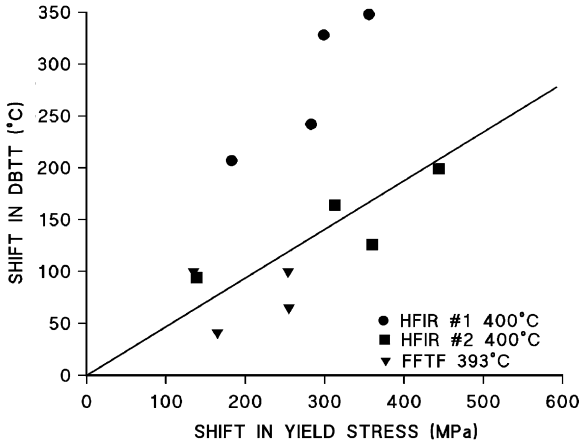

Fig. 10. Shift in ductile–brittle transition temperature plotted against the increase in yield stress for 9Cr–1MoVNb, 9Cr–1MoVNb–2Ni, 12Cr–1MoVW, and 12Cr–1MoVW–2Ni steels irradiated in the present (HFIR #2) and previous (HFIR #1) HFIR experiments at 400 °C and in FFTF at 393 °C.

to harden in accordance with the regression line. In fact, it appears that softening occurred at 400 °C for these tests relative to the recent tests. The previous results were attributed to a change in brittle fracture mode from transgranular cleavage to intergranular. This difference will be discussed in greater detail in the companion paper (Part II) [13], where mechanisms will be analyzed.

The question has been debated whether the nickel additions for the high-dose irradiations changed the microstructure to give the differences observed [14–16]. As discussed in the following section, irradiation at ≈400 °C produced a high density of fine M_6C precipitates in 9Cr–1MoVNb–2Ni and 12Cr–1MoVW–2Ni steels during irradiation in FFTF, where little helium formed, and in HFIR, where ≈400 appm He formed [17,18]. Therefore, the extra shift in DBTT in HFIR could not be attributed to irradiation-induced precipitation.

Although a helium effect was used to explain the large deviation from the linear relationship of the 40 dpa data (Fig. 10) [5,6], the results of the present experiment then present a dilemma. In the lower-dose experiment, the steels with 2% Ni developed a larger ΔDBTT than the respective steels without the added nickel, but they did not show the large differences observed for the higher fluences in HFIR. There was also no change in fracture mode. Fig. 7 provides the limited evidence in the recent results that suggests the steels with 2% Ni hardened significantly more during HFIR irradiation than the

steels without a nickel addition. Similar excess hardening for the nickel-doped steels is not evident in FFTF. If there is no difference in precipitation between the fast and mixed-spectrum reactor, the helium generated in HFIR must play a role in the hardening for similar displacement damage in the two reactors. It needs to be emphasized, however, that this difference is small (<20%), and there is considerable scatter in the data.

If helium affects the DBTT, then there should be a correlation between ΔDBTT and helium concentration. This appears to be true for 400 °C data (Fig. 11), although the reliability of the correlation suffers from a scarcity of results on steels containing high helium concentrations.

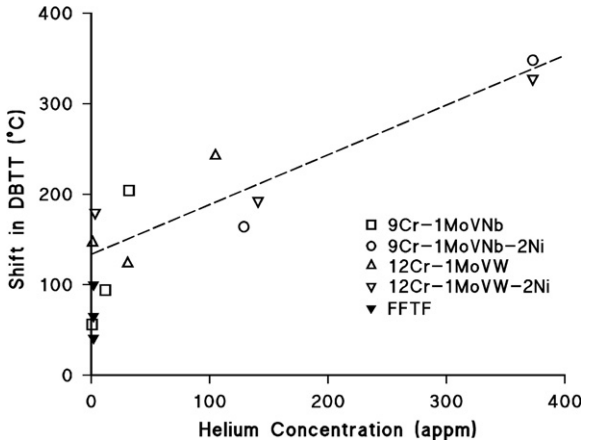

Fig. 11. Shift in ductile–brittle transition temperature plotted against helium concentration for 9Cr–1MoVNb, 9Cr–1MoVNb–2Ni, 12Cr–1MoVW, and 12Cr–1MoVW–2Ni steels irradiated in the present (HFIR #2) and previous (HFIR #1) HFIR experiments at 400 °C and in FFTF at 393 °C.

4.2. Microstructure

As pointed out in earlier papers describing irradiation experiments with the nickel-doped steels, irradiation-induced nickel-containing M_6C formed in the 9Cr–1MoVNb–2Ni and 12Cr–1MoVW–2Ni steels during HFIR irradiation to ≈40 dpa at 400 °C [17,18]. However, the same M_6C precipitates formed in irradiations of the steels to ≈47 dpa at 407 °C in the fast reactor FFTF (Fig. 12) [17,18]. If the precipitates caused hardening in the HFIR-irradiated steel, they should have caused a similar effect in FFTF for similar doses. Therefore, it was concluded that the larger ΔDBTT after irradiation in HFIR was due to helium, since helium formation in the nickel-containing steels irradiated in HFIR was the only obvious difference compared to irradiation in FFTF [5,6]. One difference in microstructure that was observed was that there was more void swelling in the HFIR-irradiated specimen.

The microstructural observations on 9Cr–1MoVNb–2Ni in the present experiment differed from the earlier studies, because no high number density of nickel-rich M_6C particles was observed after irradiation. Instead, M_2X particles were observed [Fig. 6(b)]. However, the presence of M_2X is not too surprising, because this precipitate is a chromium-rich nitride (basically Cr_2N) with some of the chromium replaced by other solutes and some nitrogen replaced by carbon. It can form more easily in 9Cr–1MoVNb steel because the specification for this steel includes 0.03–0.07% N, and the 9Cr–1MoVNb and 9Cr–1MoVNb–2Ni steels in this experiment contained 0.05% N (Table 1). Because of the relatively large size and small number density of M_2X precipitates, it would not be

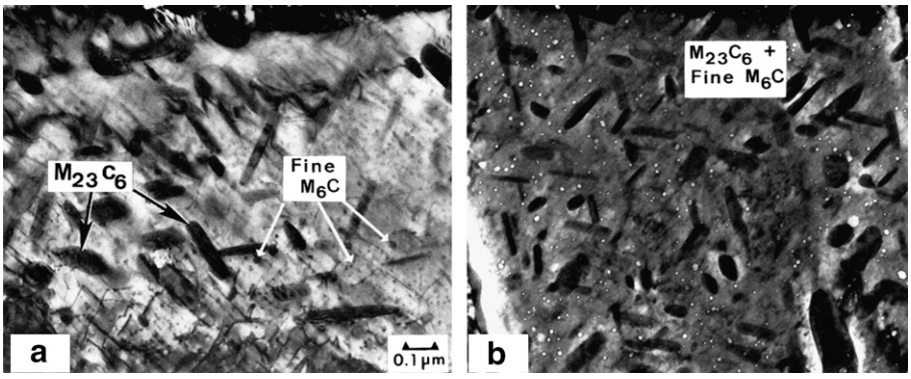

Fig. 12. Transmission electron micrographs of 9Cr–1MoVNb–2Ni steel irradiated in (a) FFTF to ≈47 dpa and ≈5 appm He and (b) HFIR at 400 °C to ≈37 dpa and ≈410 appm He.

expected to contribute much to hardening. A similar precipitation sequence should also occur for irradiation to a similar dose in FFTF.

A possible explanation for the absence of M_6C in the irradiated 9Cr–1MoVNb–2Ni, as observed in higher-dose irradiations [17,18], is that M_2X is an intermediate phase, or the small amounts present can form more quickly, and more time – a higher irradiation dose – is required for M_6C to form in sizes that can be observed and identified. Irradiations were to ≈40 dpa and higher where M_6C was observed, compared to about 12 dpa for the steels irradiated in the present experiment. The M_6C was previously analyzed as being rich in Cr, Ni, and Si, along with some iron and traces of Mo, P, and V [17,18]. A similar precipitate was detected in 12Cr–1MoVW steel irradiated in EBR-II, but in that case it was identified as G-phase, and for that steel the precipitate composition was determined as Ni–24.1Fe–12.7Si–8.7Mn–3.8Mo–1.9Cr [19].

In the irradiation capsule used for the present HFIR experiment, the reduced-activation steel 9Cr–2WVTa and that steel with 2% Ni (9Cr–2WVTa–2Ni) were also irradiated [20]. Before irradiation, the microstructures of these steels were respectively similar to those of 9Cr–1MoVNb and 9Cr–1MoVNb–2Ni – tempered martensite with $M_{23}C_6$ and MX precipitates. Likewise, there was only a minor difference in the dislocation loop structure after irradiation. However, the 9Cr–2WVTa–2Ni contained a high number density (2×10^{21} m^{-3}) of small (average size 7 nm) irradiation-induced particles identified as M_6C (Fig. 13). The size was less and the number density higher than for M_2X in 9Cr–1MoVNb–2Ni (54 nm and 5×10^{20} m^{-3}) [compare Figs. 13 and 6(b)]. Based on the above hypothesis, the absence of M_2X in the 9Cr–2WVTa is not unexpected, since this steel contains only about 0.01% N. The microstructure of 9Cr–2WVTa–2Ni was similar to structures found for 9Cr–1MoVNb–2Ni after higher-dose irradiations, supporting the hypothesis concerning the kinetics of M_6C formation in 9Cr–1MoVNb–2Ni.

4.3. Problems with nickel doping

There has been concern about using nickel-doped steels to determine helium effects, because of the effect nickel might have on the microstructure and mechanical properties [21–25]. Excess hardening in terms of an increased yield stress was observed on the reduced-activation steel JLF-1 (9Cr–2WVTa)

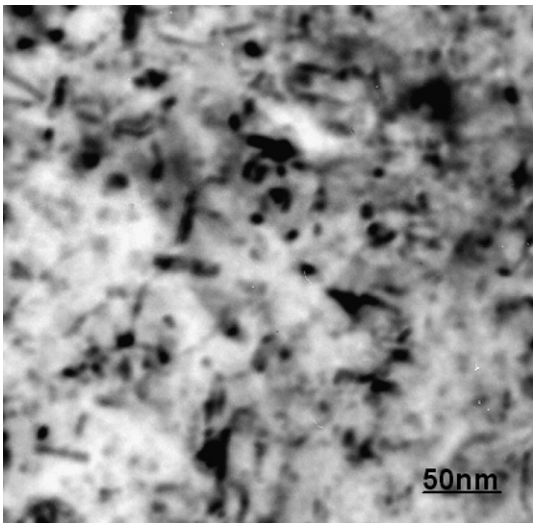

Fig. 13. Irradiation-induced M_6C precipitates in the matrix of 9Cr–2WVTa–2Ni steel irradiated in HFIR to 12 dpa at 400 °C. Compare with Fig. 6(b) that shows 9Cr–1MoVNb–2Ni irradiated similarly but containing irradiation-induced M_2X.

containing 1% Ni relative to the undoped steel after irradiation to ≈0.15 dpa at 170 °C in the Japan Materials Test Reactor (JMTR) [23,24]. No excess hardening was observed for similar irradiation at 220 °C. Irradiation of these steels in the Advanced Test Reactor (ATR) to 2.2 and 3.8 dpa at 270 and 348 °C, respectively, produced excess hardening (up to 350 MPa) for the 270 °C irradiation. Similar strengths were observed for the two steels irradiated at 348 °C [25]. The excess hardening was accompanied by a larger increase in DBTT for the nickel-containing steel.

Microstructural observations by TEM revealed that irradiation-induced dislocation loops were finer and denser in the 1% Ni steel than in the undoped steel, which suggested that the nickel addition affected nucleation and growth of dislocation loops to produce excess hardening and embrittlement [25]. Little difference in loop structure was observed in the TEM studies on the 9Cr steels irradiated in HFIR at 400 °C to 12 dpa. Likewise, no hardening attributable to nickel was observed previously for neutron irradiations of the nickel-doped 9Cr–1MoVNb and 12Cr–1MoVW steels at 300 and 400 °C [1–3], temperatures above those where the excess hardening was observed in JMTR and ATR [22–25].

In dual ion-beam irradiations (6.4 MeV Fe^{3+} and degraded 1 MeV He^{+}) to 5 dpa of F82H without nickel and with 1% and 2% Ni, hardness

measurements by an ultra-microindentation technique indicated excess hardening in the 2% Ni irradiated at 350 °C [26]. However, it is unclear how this might compare with neutron irradiation, since ion irradiations are at a dose rate several orders of magnitude higher than for fast reactor irradiations. Results from neutron irradiations indicated a two-step hardening-recovery process for the irradiated steels, with the second step occurring at $\gtrsim 300$ °C [23]. Presumably, recovery would proceed simultaneously with hardening during irradiation, thus explaining the effect of temperature on the excess hardening. Such recovery would not occur during ion irradiations to 5 dpa, which are completed within several hours, compared with several months for irradiation to 10 dpa and higher. Nevertheless, the possibility of excess hardening for the 300 °C tests must be kept in mind when evaluating these results, since there are no FFTF experiments at this temperature to determine the effect of the nickel.

4.4. Helium effects

As with all irradiation experiments, the results of this experiment involve uncertainty introduced by the small number of tests (due to limited reactor space for inserting specimens). Within the limits of such uncertainties, the present results lead to some conclusions concerning the effect of helium on mechanical properties. If similar displacement damage and precipitation occurs in the steels irradiated in FFTF and HFIR at similar temperatures, as previously observed [17,18], then the results from the present irradiations indicate there was a component of hardening that must be attributed to helium. It therefore follows that this hardening produced an increment of increase in transition temperature in the Charpy tests over and above the hardening caused by displacement damage and any irradiation-induced precipitation. Mechanisms for how helium may affect hardening will be discussed in part II [13].

Several investigators have published studies providing evidence for a helium effect on the mechanical properties of irradiated steels using other experimental techniques other than nickel doping. Also, as discussed above, the results of the present work showing a hardening effect due to helium differ from the previous high-dose experiments, where embrittlement occurred without an increase in hardness that could be attributed to helium [6,7]. In part II that accompanies this contribution, the present results will be examined in light of the previous experiments [13].

5. Summary and conclusions

The 9Cr–1MoVNb and 12Cr–1MoVW steels and these steels with 2% Ni additions were irradiated in HFIR to ≈10 dpa at 300 °C and ≈12 dpa at 400 °C and in FFTF to ≈15 dpa at 393 °C. After irradiation in HFIR, steels with 2% Ni hardened more than steels without a nickel addition. When 9Cr–1MoVNb–2Ni, 12Cr–1MoVW, and 12Cr–1MoVW–2Ni steels were irradiated in HFIR at 400 °C, they hardened more than when irradiated in FFTF at 393 °C. The 9Cr–1MoVNb steel hardened to the same level in both FFTF and HFIR. For all but the 9Cr–1MoVNb steel, shifts in DBTT of the steels irradiated in HFIR were greater than shifts for the same steels irradiated in FFTF. Irradiation in HFIR at 300 and 400 °C caused a larger shift for the steels containing 2% Ni than for the steels with no nickel addition. The increase in DBTT was related to the increase in yield stress. Despite the uncertainty inherent in the experiments, the results lead to the conclusion that helium caused an increment of hardening that contributed to the extra shift in DBTT over that observed after irradiation in FFTF where little helium formed.

Acknowledgements

We wish to thank the following people who helped in the completion of this work: L.T. Gibson, N.H. Rouse, and E. T. Manneschmidt carried out the experimental tests and procedures; Dr L.R. Greenwood analyzed the dosimetry specimens in the irradiation capsules and calculated the helium concentrations; Drs D.R. Harries, L.K. Mansur, R.G. Stoller, and S.J. Zinkle reviewed the manuscript and provided helpful discussion of the work.

This research was sponsored by the Office of Fusion Energy Sciences, US Department of Energy, under contract DE-AC05-00OR22725 with U.T. Battelle, LLC.

References

[1] R.L. Klueh, P.J. Maziasz, J.M. Vitek, J. Nucl. Mater. 141–143 (1986) 960.
[2] R.L. Klueh, J.M. Vitek, J. Nucl. Mater. 150 (1987) 272.
[3] R.L. Klueh, P.J. Maziasz, J. Nucl. Mater. 187 (1992) 43.
[4] J.M. Vitek, W.R. Corwin, R.L. Klueh, J.R. Hawthorne, J. Nucl. Mater. 141–143 (1986) 948.

[5] W.R. Corwin, J.M. Vitek, R.L. Klueh, J. Nucl. Mater. 149 (1987) 312.
[6] R.L. Klueh, D.J. Alexander, J. Nucl. Mater. 187 (1992) 60.
[7] R.L. Klueh, D.J. Alexander, J. Nucl. Mater. 218 (1995) 151.
[8] D.J. Alexander, R.K. Nanstad, W.R. Corwin, J.T. Hutton, in: A.A. Braun, N.E. Ashbaugh, F.M. Smith (Eds.), Applications of Automation Technology to Fatigue and Fracture Testing, ASTM STP, vol. 1092, American Society for Testing and Materials, Philadelphia, 1990, p. 83.
[9] M.A. Sokolov, R.K. Nanstad, in: D.S. Gelles, R.K. Nanstad, A.S. Kumar, E.A. Little (Eds.), Effects of Radiation on Materials: 17th International Symposium, ASTM STP, vol. 1270, American Society for Testing and Materials, Philadelphia, 1996, p. 384.
[10] N. Hashimoto, R.L. Klueh, J. Nucl. Mater. 305 (2002) 153.
[11] W.C. Leslie, The Physical Metallurgy of Steels, McGraw-Hill, New York, 1981, p. 123.
[12] W.L. Hu, D.S. Gelles, in: F.A. Garner, C.H. Henager Jr., N. Igata (Eds.), Influence of Radiation on Material Properties: 13th International Symposium (Part II), ASTM STP, vol. 956, American Society for Testing Materials, Philadelphia, 1987, p. 83.
[13] R.L. Klueh, N. Hashimoto, M.A. Sokolov, K. Shiba, S. Jitsukawa, J. Nucl. Mater. to be published.
[14] D.S. Gelles, J. Nucl. Mater. 230 (1996) 187.
[15] R.L. Klueh, D.J. Alexander, J. Nucl. Mater. 230 (1996) 191.
[16] N. Hashimoto, R.L. Klueh, J. Nucl. Mater. 305 (2002) 153.
[17] P.J. Maziasz, R.L. Klueh, J.M. Vitek, J. Nucl. Mater. 141–143 (1986) 929.
[18] P.J. Maziasz, R.L. Klueh, in: N.H. Packen, R.E. Stoller, A.S. Kumar (Eds.), Effects of Radiation on Materials: 14th International Symposium, ASTM STP, vol. 1046, American Society for Testing and Materials, Philadelphia, 1990, p. 35.
[19] D.S. Gelles, L.E. Thomas, in: J.W. Davis, D.J. Michel (Eds.), Ferritic Steels for use in Nuclear Energy Technologies, The Metallurgical Society of AIME, Warrendale, PA, 1984, p. 559.
[20] R.L. Klueh, M.A. Sokolov, K. Shiba, Y. Miwa, J.P. Robertson, J. Nucl. Mater. 283–287 (2000) 478.
[21] D.S. Gelles, G.L. Hankin, M.L. Hamilton, J. Nucl. Mater. 251 (1997) 188.
[22] D.S. Gelles, in: R.K. Nanstad, M.L. Hamilton, G.A. Garner, A.S. Kumar (Eds.), Effects of Radiation on Materials: 18th International Symposium, ASTM STP, vol. 1325, American Society for Testing and Materials, Philadelphia, 1997, p. 899.
[23] R. Kasada, A. Kimura, H. Matsui, M. Narui, J. Nucl. Mater. 258–263 (1998) 1199.
[24] R. Kasada, T. Morimura, H. Matsui, M. Narui, A. Kimura, in: M.L. Hamilton, A.S. Kumar, S.T. Rosinski, M.L. Grossbeck (Eds.), Effects of Radiation on Materials: 19th International Symposium, ASTM STP, vol. 1366, American Society for Testing and Materials, West Conshohocken, PA, 2000, p. 448.
[25] R. Kasada, A. Kimura, Mater. Trans. 46 (2005) 475.
[26] M. Ando, H. Tanigawa, S. Jitsukawa, T. Sawai, Y. Katoh, A. Kohyama, K. Nakamura, H. Takeuchi, J. Nucl. Mater. 307–311 (2002) 260.